Cooperative Phenomena below Melting of the One-Component Two-Dimensional Plasma

Ph. Choquard
Institut de Physique Théorique, Ecole Polytechnique Fédérale de Lausanne, CH-1015 Lausanne, Switzerland

and

J. Clerouin [a]
Equipe de Recherche Physique Mathématique, Modélisation et Simulation, F-45045 Orleans-Cédex, France

(Received 22 April 1983)

This Letter reports investigations by molecular dynamics of the melting transition of a two-dimensional one-component plasma consisting of 511 particles with logarithmic interactions confined to a disk. Evidence is presented for a weak first-order transition occurring at $T_m = e^2/k\Gamma_m$ with $\Gamma_m \simeq 142$ and with a melting entropy $\simeq 0.17$ K. This small entropy is attributed to important premelting phenomena which are cooperative, cyclic permutations of six and more particles as revealed by labeling experiments.

PACS numbers: 64.70.Dv, 52.25.Kn, 61.20.Ja

The first investigation by molecular dynamics of the melting transition of the two-dimensional one-component plasma (2D-OCP) was carried out by de Leeuw and Perram.[1] Using periodic boundary conditions, they reported strong evidence of a first-order transition occurring at $\Gamma_m \simeq 135$. A value of $\Gamma_m \simeq 140$ has been obtained by Caillol *et al.*[2] They compared the free energy of the harmonic crystal with the free energy resulting from integrating internal energies from a Monte Carlo simulation of particles confined to the surface of a sphere with respect to Γ starting from the $\Gamma = 2$ result. Using for the fluid phase a careful extrapolation of the free energy calculated for a small number of particles confined to a disk, Johannesen and Merlini[3] gave an estimate of $\Gamma_m \simeq 137$. In this Letter, we report extensive molecular dynamics investigations of the coexistence and premelting regions for the 2D-OCP. Following individual particle histories shows the importance of cooperative motions, strikingly reminiscent of phenomena occurring in hard-disk systems as recently reviewed by Alder, Ceperly, and Pollock.[4]

The OCP model consists of an assembly of charged point particles immersed in a neutralizing background. In two dimensions, the Coulomb potential between two particles of charge e and separated by a distance $r = |\vec{r}|$ is $-e^2 \ln(r/L)$, where L is a scaling length. For a neutral system of N particles confined in a disk of radius R, the potential energy is[5]

$$V = -e^2 \sum_{i<j} \ln\left(\frac{r_{ij}}{R}\right) + \frac{Ne^2}{2} \sum_i \left(\frac{r_i}{R}\right)^2 - \tfrac{3}{8} N^2 e^2 - \frac{Ne^2}{2} \ln\left(\frac{L}{R}\right),$$

where r_i is the position of particle i and $r_{ij} = |\vec{r}_i - \vec{r}_j|$. Our simulations are performed with free boundary conditions on the disk. The simplicity of the corresponding Hamiltonian makes very fast calculations possible, particularly at low temperature where the kinetic pressure turns out to be vanishingly small. The number of particles is chosen from a sequence such that the neutralizing disk accommodates exactly a perfect triangular lattice of particles centered at the origin of the disk. This sequence has been investigated by Sari, Merlini, and Calinon.[5] $N = 511$ is the number from this sequence which best fits our computing facilities. While the Madelung energy is $-0.3744e^2$, the energy per particle of this crystal is $-0.3652e^2$. Relaxation of the system toward its configuration of minimum energy yields an energy per particle of $-0.3727e^2$, but this is accompanied by a strong deformation of the outer shells of particles due to the circular boundary conditions. In order to avoid this effect, we have pinned the twelve particles of the outermost shell at their ideal lattice positions. Subsequently relaxing the other 499 particles gives the ground-state configuration of our system with an energy per particle of $-0.3692e^2$.

The initial molecular dynamics simulation is started from the ground-state spatial configuration by giving the particles velocities chosen at random from a Maxwellian distribution. Verlet's algorithm is used with time steps $\Delta t = 0.22/\omega_p$, ω_p being the natural plasma frequency, and with free boundary conditions at the edge of the disk. Structural properties are measured in a subdisk of radius $R/2$, in order to avoid boundary effects. Studies at subsequent energies are started from

the final spatial configuration of an earlier run, with the velocities rescaled to change the total energy. As a result of the long-range Coulomb potential, it is necessary to compute explicitly all the $N(N-1)/2$ interactions among the particles at each time step. This is the most time consuming part of the computer program (99.17%). The twelve pinned particles take part in the force field but do not move.

Figure 1 displays the mean kinetic energy, identified with kT, versus the energy per particle. The gross features observed are a solid and a fluid branch with a changeover occurring at $kT_m \simeq e^2/142$. The results of de Leeuw and Perram and of Caillol *et al.* are included for comparison. The shift of de Leeuw and Perram's results to lower energy is caused by the potential-energy difference between periodic and free boundary conditions with pinned particles, but this difference does not explain entirely the smaller size of our transition region, nor the fact that we observe little hysteresis. The inverse slope of the two straight-line segments on the graph is 2, corresponding exactly to the law of Dulong and Petit. Note that the Monte Carlo data of Caillol *et al.* show no discontinuity but reveal instead a low-temperature Wigner glasslike state compatible with the topology of their system.

The structural properties of the two phases are exhibited by the pair distribution function $G(\vec{r})$ illustrated in Fig. 2 for four values of the energy. The crystalline and isotropic liquid nature of the two branches appears clearly at the points labeled $S1$ and $L3$. At the point $S3$ which is very close to the changeover, the crystalline structure still persists. At the point $L2$ which lies just above the transition, $G(\vec{r})$ is anisotropic. Its orientation seems to fluctuate slightly with time and independently of the orientation induced by the pinned particle field. However, this anisotropic phase may be an artifact of the finite size of the system. From the complete pair distribution function it is customary to extract the radial dependence, $g(r)$, by angular averaging of $G(r, \theta)$. This $g(r)$ yields the standard shell structure of crystals and liquids. In a two-dimensional system, however, the knowledge of the angular part, $\bar{g}(\theta)$, obtained by radial averaging of $G(r, \theta)$, is of central interest: It is the signature of orientational order in the system. Inspection of the changes in our $\bar{g}(\theta)$ across the transition shows the disappearance of the long-range orientational order at $\Gamma \simeq 142$. With use of $g(r)$ and $\bar{g}(\theta)$ it is possible to analyze the latter in terms of contributions arising from successive shells, i.e., $\bar{g}(\theta) = \bar{g}_1(\theta) + \bar{g}_2(\theta) + \ldots$. Short-range orientational order is essentially determined by $\bar{g}_1(\theta) = \int_0^{R_1} G(r,$

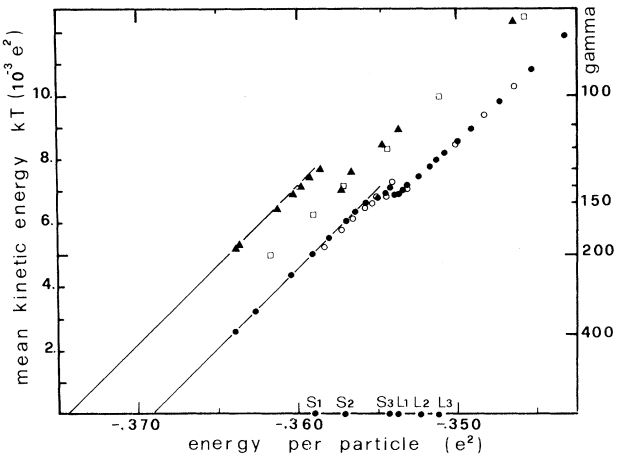

FIG. 1. Mean kinetic energy vs energy per particle. Solid points correspond to heating-up and open circles to cooling-down experiments, each of 6000 time steps. Triangles are the data of de Leeuw and Perram and squares are the data of Caillol *et al.* $S1, S2, S3$, and $L1, L2, L3$ are points in the solid and in the fluid phase studied in detail. Straight lines correspond to the harmonic approximation.

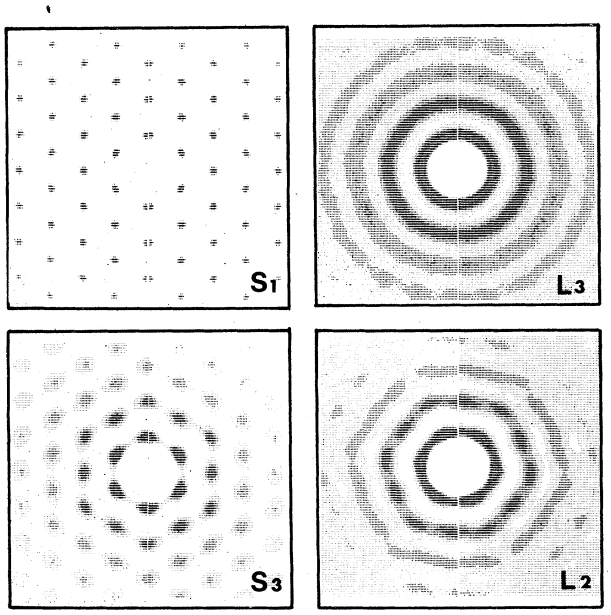

FIG. 2. Pair distribution function $G(\vec{r}) \equiv G(r, \theta)$ for the four points $S1$, $S3$, $L2$, and $L3$ corresponding, respectively, to the energies $-0.3591e^2$, $-0.3542e^2$, $-0.3525e^2$, and $-0.3512e^2$ or to $\Gamma \simeq 200$, $\Gamma \simeq 140$, $\Gamma \simeq 137$, and $\Gamma \simeq 125$. These figures represent averages over 10 000 time steps.

$\theta) r\,dr$ where R_1 is the position of the first nontrivial minimum of $g(r)$.

In order to examine more closely the nature of the melting transition, we have picked several energies around $S3$ and $L1$. Characteristic pictures of the particle trajectories reveal solid-liquid phase coexistence unambiguously. The solid and liquid coexist at the same density and mean kinetic energy, but their mean potential energies differ. As the energy is increased from the beginning to the end of the coexistence region the liquid takes up the excess energy as potential energy. This analysis is consistent with the microcanonical description of the transition. Although our latent heat of fusion ($0.0012e^2$) is significantly smaller than that of de Leeuw and Perram ($0.0027e^2$), we still conclude that the melting transition is first order. We can furthermore interpret $S3$ as a superheated crystal and $L1$ as a supercooled liquid.

A detailed study of the premelting region has been carried out. We have plotted in Fig. 3 the mean kinetic energy and the specific heat C_v versus the energy. Up to the point labeled $S2$ the system behaves as a harmonic crystal as demonstrated by the straight line $kT=\frac{1}{2}(E-U_0)$ and by a direct computation of C_v from kinetic energy fluctuations. Above $S2$ we observe a rapid growth of C_v and simultaneously a slow divergence of Lindemann's ratio. This is a signal of particle excursions from lattice cells. A labeling experiment has been set up to detect systematically the occurrence and the nature of these motions. Figure 4 shows for the points labeled a, b, c, and d (in Fig. 3) that these excursions occur typically as cooperative, cyclic permutations of 6, 8, and more particles, up to gliding of a row. It is remarkable that similar cooperative motions have been observed in hard-disk systems by Alder, Ceperly, and Pollock.[4] This suggests a deep connection between the two models which are at first sight radically different, and the possible universality of these motions in two dimensions. Note that these cyclic permuations can in principle occur at all nonzero temperatures, but their frequencies are practically vanishing below $S2$. Above this point multiplication and combination of elementary permutations occur, so that the specific heat increases while the short-range orientational order decreases. This effect can be seen in Fig. 5 which shows a plot of the peak value of $\bar{g}_1(\theta)$ as a function of the energy per particle. These observations suggest exploring the idea that the crystal melts when the difference between the free energy of a locked and a freely rotating cycle reaches zero. From our data we conclude that the phase coexistence begins at $-0.3547e^2$, ceases at $-0.3535e^2$, and that complete fluid isotropy is reached at $-0.3512e^2$. Error estimates on energies per particle for locating these particular points are $\pm 0.0001e^2$.

The results of our investigations can be summarized as follows:

(i) The 2D-OCP exhibits a weak first-order transition at $\Gamma = 142 \pm 3$ with a latent heat of fusion

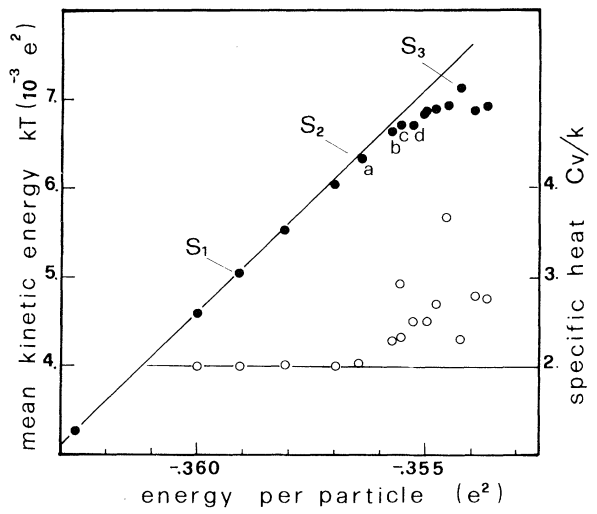

FIG. 3. Mean kinetic energy and specific heat vs energy per particle in the premelting region.

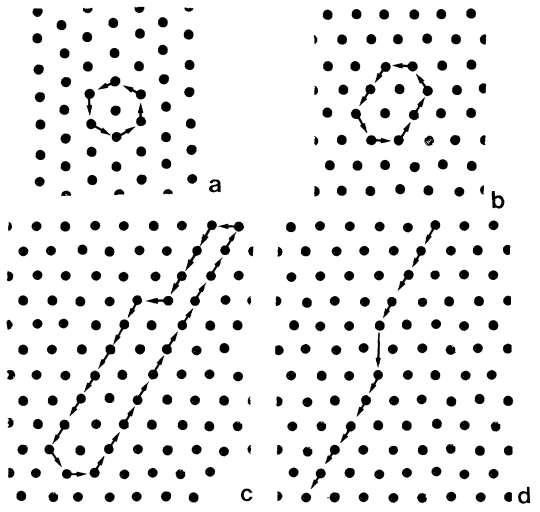

FIG. 4. Cooperative motions of particles below melting for the points labeled a, b, c, and d in Fig. 3.

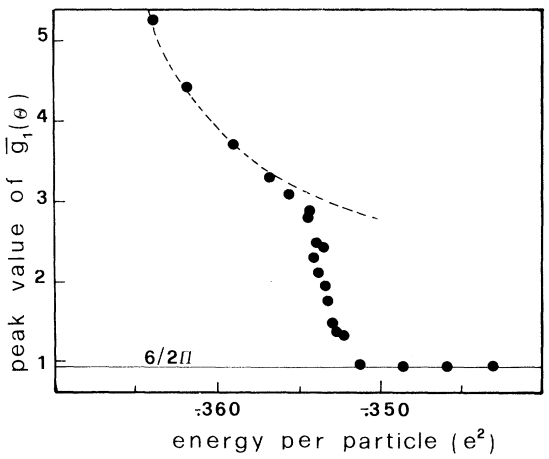

FIG. 5. Plot of the peak value of $\bar{g}_1(\theta)$ vs energy per particle. The dashed line represents the harmonic approximation. The horizontal solid line represents the isotropic fluid value.

$=(0.0012\pm0.002)e^2$ and a melting entropy $=0.17\pm0.03$ K.

(ii) The weakness of the transition is attributed to important premelting phenomena which consist of cooperative, cyclic permutations of 6, 7, 8, 9, and more particles. These motions have been revealed by our labeling experiments which we believe to be the first such experiments for a system with a soft repulsive potential.

(iii) Since similar cooperative phenomena have been observed in hard-disk systems we conjecture that they should occur in 2D weak first-order transitions in general and further that a temperature-dependent effective core diameter might usefully be introduced to simulate their steric aspect. However, more labeling experiments and more specific-heat data on other 2D systems below melting are needed to support the conjecture.

It is our intention to publish more details, particularly quantative, in a subsequent paper.

These computer experiments would not have been possible without the encouragement and assistance of A. Quignodon and of the CRAY-1 support staff of CISI/FRANLAB.

[a]Present address: Centre d'Etudes de Limeil, B.P. 27, F-94190 Villeneuve St. Georges, France.

[1]S. W. de Leeuw and J. W. Perram, Physica (Utrecht) 113A, 546 (1982).

[2]S. M. Caillol, D. Levesque, J. J. Weis, and J. P. Hansen, J. Stat. Phys. 28, 324 (1982).

[3]S. Johannesen and D. Merlini, Phys. Lett. 93A, 21 (1982).

[4]B. J. Alder, D. M. Ceperly, and E. L. Pollock, Int. J. Quantum Chem., Symp. No. 16, 49 (1982).

[5]R. R. Sari, D. Merlini, and R. Calinon, J. Phys. A 9, 1539 (1976).

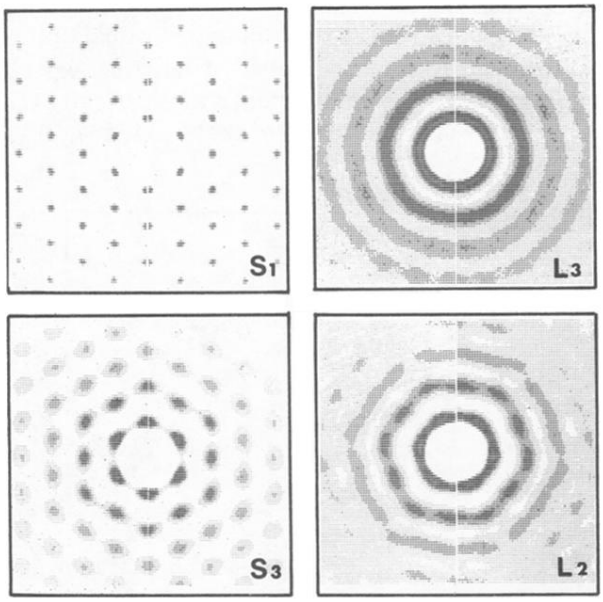

FIG. 2. Pair distribution function $G(\vec{r}) \equiv G(r, \theta)$ for the four points $S\,1$, $S\,3$, $L\,2$, and $L\,3$ corresponding, respectively, to the energies $-0.3591e^2$, $-0.3542e^2$, $-0.3525e^2$, and $-0.3512e^2$ or to $\Gamma \simeq 200$, $\Gamma \simeq 140$, $\Gamma \simeq 137$, and $\Gamma \simeq 125$. These figures represent averages over 10 000 time steps.